Infrared Variability of Long-Lived Disk Around Young M6 Dwarf

Seth Zoppelt[a,b], Michael Liu[b], Zhoujian Zhang[c]

[a]*Dept of Physics and Astronomy, College of Charleston, 66 George St, Charleston, SC 29424, USA*

[b]*Institute for Astronomy, University of Hawai'i, 2680 Woodlawn Drive, Honolulu, HI 96822, USA*

[c]*Dept of Astronomy, University of Texas at Austin, 2515 Speedway, Stop C1400, Austin, TX 78712, USA*

Abstract

Circumstellar disk formation and evolution are key steps in the formation of planets and the understanding of Young Stellar Objects (YSOs). The circumstellar disk around 2MASS J06195260-2903592, a young M6 variable star, is particularly long-lived ($\approx 30\,Myr$). Here, we present photometric data of 2MASS J0619-2903 in the J and K filters using WFCAM on UKIRT taken over several epochs from December 2021 to March 2022, allowing for a closer examination of the star's behavior across shorter timescales than previously measured (i.e., months instead of scattered data across years). With this data, we show a fully corrected light curve in each filter as well as a J-K color-magnitude plot. From these light curves and color plot, we show that this system's extinction is variable on short time scales, on the order of days.

Keywords: M dwarf stars, Circumstellar matter

1. Introduction

Circumstellar disks offer a keen insight into the formation of Young Stellar Objects (YSO) as well as to study planet formation. These disks offer an important clue into the formation of the early Solar System and how the planets formed in the Sun's protoplanetary disk. These disks are a consequence of the conservation of angular momentum (Williams & Cieza, 2011; Manara et al., 2022) around very young stars. Their timescale is $\sim 10\,Myr$ (Haisch et al., 2001; Ansdell et al., 2016) with planetary formation beginning as soon as a few Myr (Ansdell et al., 2016; Manara et al., 2022). Lada & Wilking (1984) first showed that YSOs in Ophiuchus exhibited three distinct characteristics based on whether the emitted spectral distribution energy was rising in the mid-infrared, declining but with a notable excess over the blackbody stellar atmosphere, or with negligible mid-infrared excess.

Time-series observations gather new information on the variability, structure, and dynamics that cannot be determined from a single spectral energy distribution. This information

Email address: zoppeltsa@g.cofc.edu (Seth Zoppelt)

could include disk processes, such as thermal emission from an over-dense region of the inner disk, variable disk accretion, some structure in the disk rotating in and out of view, or disk instabilities (Fedele et al. (2007); Plavchan et al. (2008); Herbst et al. (2010); Plavchan et al. (2013); Rebull et al. (2014)).

2MASS J0619-2903 was discovered by Cruz et al. (2003) and first identified by Liu, Dupuy & Allers (2016) as an unusual field object due to its strong IR excess and variable NIR spectrum. Allers & Liu (2013) classified the near-IR 2MASS J0619-2903 as M5. Unlike most YSOs, 2MASS J0619-2903 has an unusually long-lived circumstellar disk ($\approx 30\,Myr$). Silverberg et al. (2020) coined the term "Peter Pan" disks for very old ($\gtrsim 20\,Myr$) disks with strong infrared excess around young M dwarfs. In order for these disks to live this long, there must be some rare properties associated with the disk, such as low disk viscosity, extremely low external photoevaporation (indicating formation in rare environment), or relatively high disk masses (Coleman & Haworth, 2020).

The goal of this paper is to further examine the variability of 2MASS J0619-2903 using UKIRT near-IR photometry (see section 2). Since we have data across multiple epochs, we are able to construct a more precise light curve to examine 2MASS J0619-2903's variable properties. In particular, we have data taken across multiple consecutive nights, for a more thorough understanding of the variability of the star across a monthly period, rather than across years or sporadically across some nights as used in Liu et al. (2022, submitted). Sections 3 and 4 provide the light curves, results of the light curves, and discussion.

2. Method

Our data were taken via the Wide Field CAMera (WFCAM) (see Figure 1) on UKIRT using a 9-point grid pattern and two filters, J and K. The images were taken with 60 second exposures across a period of about 3 months. All data was processed using the VISTA Data Flow System (VDFS), run by QMUL, Cambridge, and Edinburgh (Lawrence et al., 2007). The system removes instrumental signatures, extracts source catalogues on a frame by frame basis, constructs survey level products, and provides the data to the user(s).

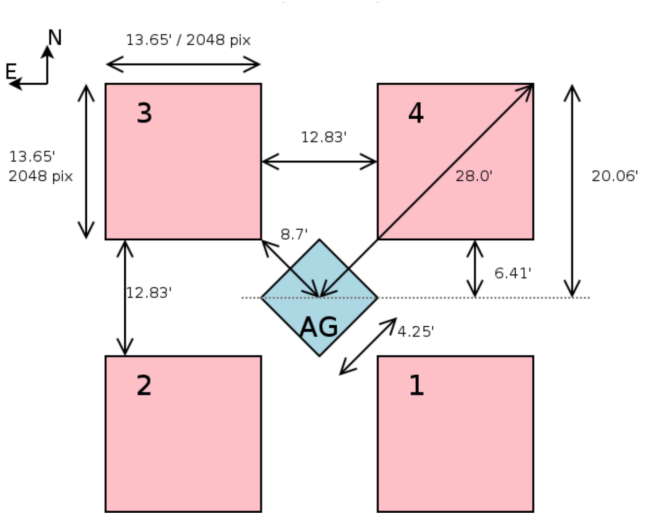

Figure 1: Schematic of WFCAM detector. Our object, 2MASS J0619-2903 resides in quadrant 3. The arrays are spaced such that 4 separate observations can be tiled to cover 0.75 deg^2 of the sky, with a single exposure covering 0.19 deg^2 with 0.4″ pixels (Casali et al., 2007).

Since UKIRT is a queue-scheduled telescope, the seeing was not always great during observations. (Figure 2). For reference, the seeing on Mauna Kea can be as good as 0.4″. The zero point, (Figure 3), has much less scatter, but there were some observations in the K filter and ~ 1 observation in the J filter that had zero point values $< 21\, mag$, much less than the typical value shown for the images. These values also correspond to the larger errors seen in Figure A.1.

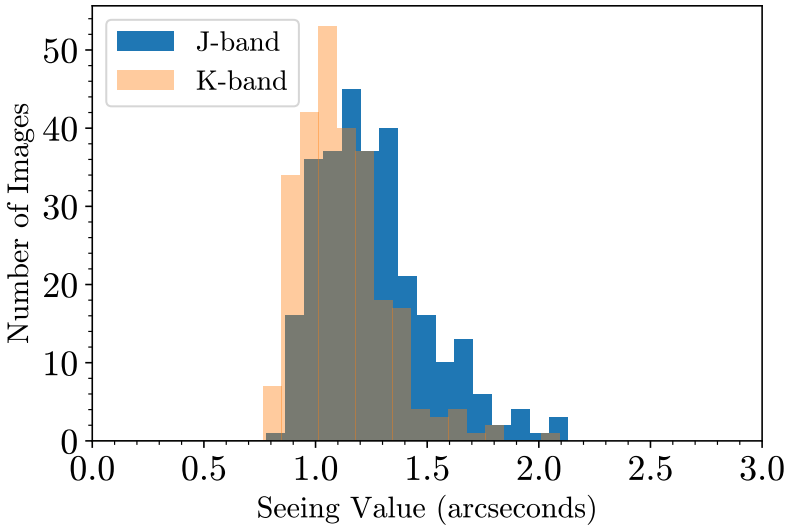

Figure 2: Seeing values here are defined as the average of the FWHM across the image (in pixels). The values were multiplied by 0.4 to convert to arcseconds. The values were collected with each image from each observation run. Since these observations were taken on nights with poorer seeing, the seeing values are much larger than what would typically be expected on the Maunakea summit. The slight skew toward better values seen in the K filter could be due to typically better seeing values for larger wavelengths.

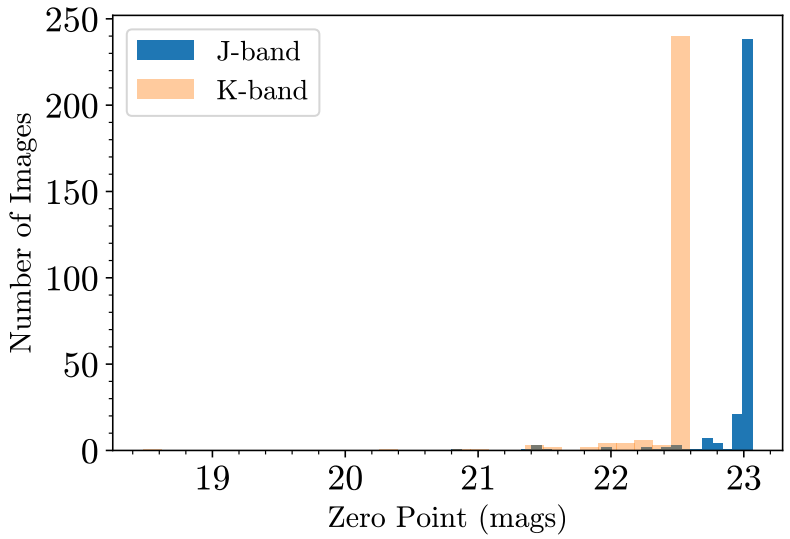

Figure 3: Zero point values collected during each observation run (separated for J- and K- filters). A zero point value was collected for each image taken, and the value was recorded in the header of each FITS image catalog.

2.1. Reference Star Selection and Calibration Curve

In order to correct light curves to remove background noise, possible fluctuations in the instrument, etc., a normalized flux curve is needed. This flux curve is used to divide this

noise, background light, etc. to create the final calibration curve (Figure 4). This calibration curve can then be used to create finalized light curves (Figures 5 and 6).

In order to create the calibration curve seen in Figure 4, 29 stars in the 2MASS catalog were selected (Table 1). These stars were selected because they were within $2\,arcmin$ of our target, and all stars had J- and K-magnitudes within $\pm 3\,mags$. The reference curves were created by median combining all reference star curves. Then, a weighted average was taken for each star, and they were further combined again to produce the final normalized curve. From there, the final calibrated curve was created (Figure 4). The final calibration curves in Figure 4 had some odd outlier points in both filters, which are most likely a consequence of poor data.

Star (2MASS)	J mag	K mag
06194883-2904512	12.799	11.890
06195881-2903454	13.202	12.887
06194493-2903384	13.673	12.909
06195174-2905098	13.718	13.376
06194897-2905467	14.003	13.602
06195219-2903439	14.370	13.677
06195289-2903205	14.659	14.306
06195460-2905454	15.123	14.740
06195195-2905414	15.165	14.463
06194648-2903473	15.187	14.576
06195267-2902356	15.265	14.383
06195526-2903504	15.388	14.953
06194914-2903317	15.467	15.124
06195478-2905405	15.941	15.202
06195471-2904374	15.976	14.997
06195638-2903429	16.118	14.992
06195471-2904438	16.136	15.442
06194664-2904479	16.187	15.483
06195671-2902312	16.480	15.542
06195886-2903347	16.573	15.522
06200000-2903200	16.603	15.021
06194624-2903149	16.617	16.103
06195166-2903505	16.620	15.650
06195827-2904046	16.756	15.762
06194910-2903389	16.761	16.253
06194757-2903234	16.822	15.550
06194980-2905235	16.826	15.142
06195359-2905103	17.120	15.671
06195338-2904512	17.252	15.743

Table 1: All reference stars chosen along with corresponding J- and K-magnitudes. All stars here were used to create the calibration curves in each respective filter seen in Figure 4.

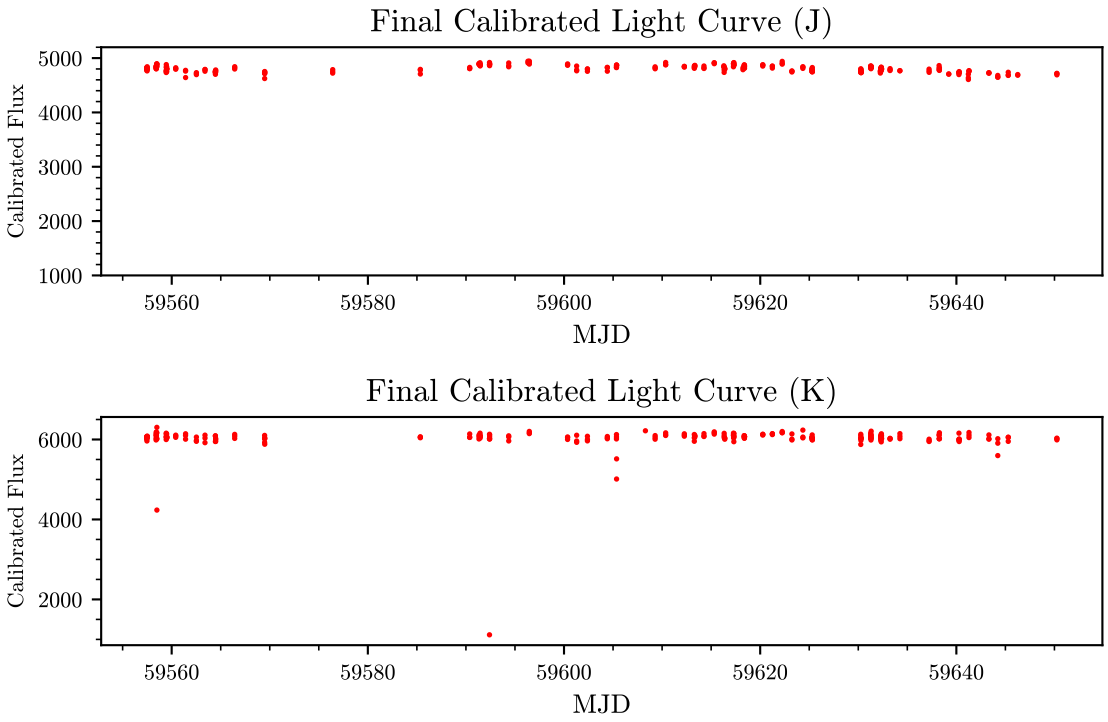

Figure 4: Final calibrated curves for the J filter (top plot) and K filter (bottom plot). The in the K curve most likely arise from poorer viewing conditions. See Figure 7 for the final light curve in the K filter.

3. Results and Discussion

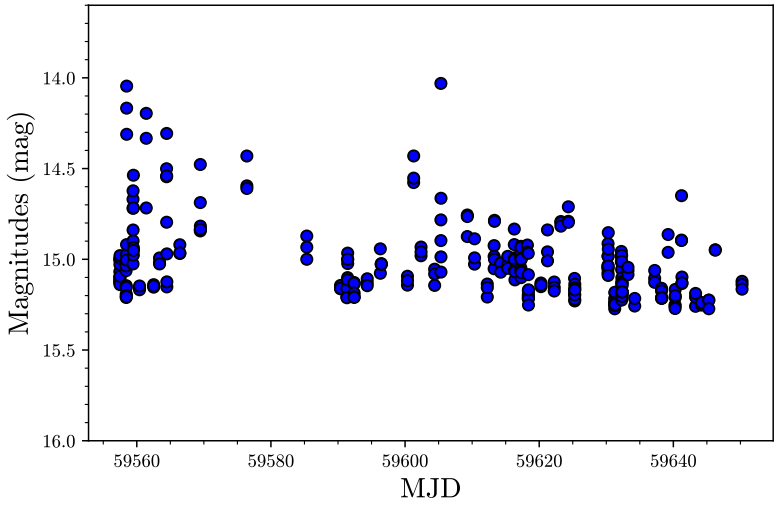

Figure 5: Light curve for 2MASS J0619-2903 in the J filter. The errors were small enough ($\sim 0.01\,mag$) that they are barely resolvable. Some notable spikes, such as the ones at about MJD 59560, 59600, and 59640, suggest variability on this days-long timescale. More on this variability will be discussed below.

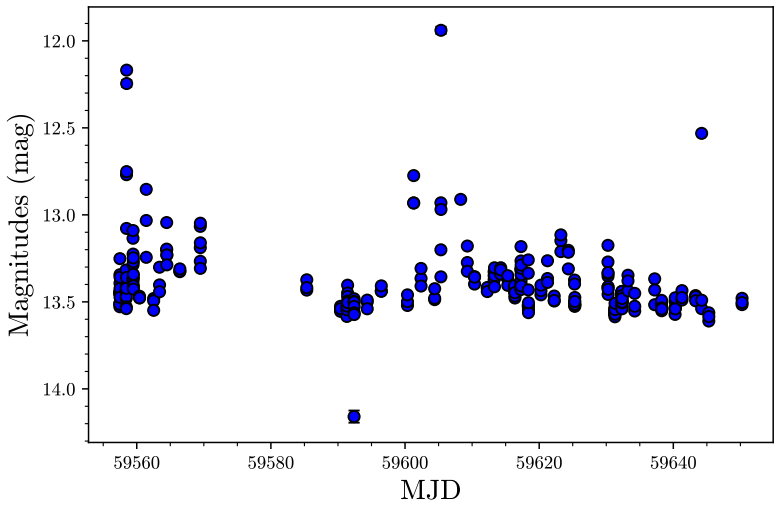

Figure 6: Light curve for 2MASS J0619-2903 in the K filter. The spikes seen around similar MJDs as in Figure 5 further suggest variability at this filter wavelength as well. The single point below $14.0\,mag$ is not an artifact of the variability of this system; rather, it is most likely a consequence of poor data.

Figures 5 and 6 show the final light curves for 2MASS J619-2903. Some of these data were removed due to very poor image quality, assessed by visually examining the images with DS9. These light curves here show evident variability. This variability could be a result of

extinction from the disk as it orbits the star and obscures our field of view as well as from the star itself. The variability is prominent on shorter timescales than previously observable, on the order of days. This impressive variability demonstrates the ever-changing conditions around YSOs and 2MASS J0619-2903.

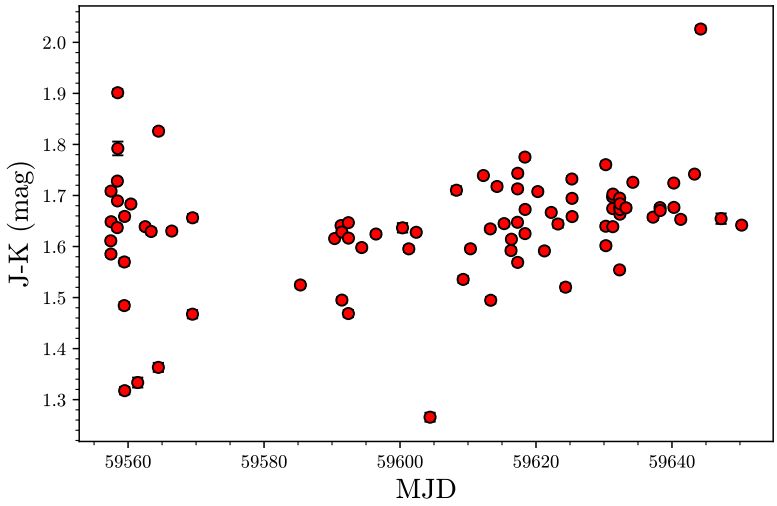

Figure 7: Shown is the J-K Color-Magnitude plot for 2MASS J0619-2903. The error is small enough ($\sim 0.01\,mag$) that it is barely resolvable. The color is changing almost constantly and rapidly (within a couple days of consecutive observations). This suggests that there is much extinction between the star and our line of sight, potentially caused by obscuration of the disk through our line of sight.

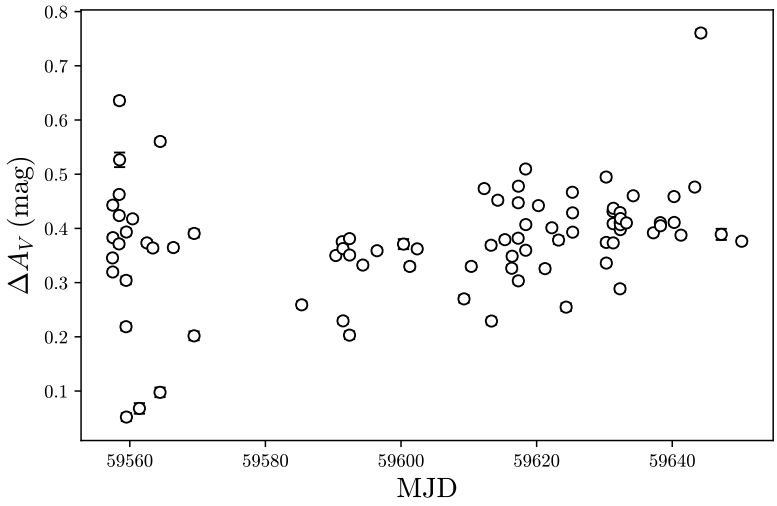

Figure 8: ΔA_V plot for 2MASS J0619-2903. This plot was generated by subtracting each value from the bluest point in Figure 7, which is $J-K = 1.265\,mags$. Here, there is evident extinction as well as variability in the extinction as well across near-consecutive days.

Figure 7 shows the J-K color-magnitude plot and Figure 8 shows the ΔA_V plot, a way to view possible extinction from the disk around the star. The ΔA_V plot was created by taking the bluest point in Figure 7 and subtracting from other points also in that plot. There is also much variability in the plot, which could suggest much variability in the composition, viscosity, and density of the disk. This large variability in the plot over short timescales (across just mere days or even hours) shows the large variation of the disk as it orbits.

4. Conclusions

In this paper, we showed a full analysis and creation of two light curves for the young M6 dwarf 2MASS J06195260-2903592 as well as a J-K color-magnitude plot. These plots confirmed that there is massive variability around the star, and there is clearly extinction occurring around the disk at much shorter timescales (i.e., days and weeks) than previously observed (Liu et al. (2021, submitted). The disk, as it orbits, exhibits varying densities and has a definite presence, marking it as a very long-lived circumstellar disk ($\approx 30\,Myr$).

Software

This project would not be possible without the Astropy package in Python (Astropy Collaboration et al. (2013), Astropy Collaboration et al. (2018), The Astropy Collaboration et al. (2022)). Numpy 1.21.2 (Harris et al., 2020).

Acknowledgements

This project would not be possible without the Astropy package in Python (Astropy Collaboration et al., 2018). This research has made use of the VizieR catalogue access tool, CDS, Strasbourg, France (DOI : 10.26093/cds/vizier). The original description of the VizieR service was published in 2000, AAS 143, 23. In this catalog, the 2MASS all-sky catalog of point sources was also used (Cutri et al., 2003) Seth Zoppelt acknowledges support from Research Experience for Undergraduate program at the Institute for Astronomy, University of Hawaii-Manoa funded through NSF grant #2050710. Seth Zoppelt would like to thank the Institute for Astronomy for their hospitality during the course of this project. This work is based on observations made by UKIRT. We wish to extend our special thanks to those of Hawaiian ancestry on whose sacred mountain of Maunakea we are privileged to be guests. The observations presented herein would not have been possible without their generosity. Seth Zoppelt would like to greatly thank his mentor and co-author, Dr. Michael Liu for pushing him to become an even better researcher.

References

Allers, K. N., & Liu, M. C. 2013, The Astrophysical Journal, 772, 79, doi: http://doi.org/10.1088/0004-637x/772/2/7910.1088/0004-637x/772/2/79

Ansdell, M., Williams, J. P., van der Marel, N., et al. 2016, The Astrophysical Journal, 828, 46, doi: http://doi.org/10.3847/0004-637x/828/1/4610.3847/0004-637x/828/1/46

Astropy Collaboration, Robitaille, T. P., Tollerud, E. J., et al. 2013, A&A, 558, A33, doi: http://doi.org/10.1051/0004-6361/20132206810.1051/0004-6361/201322068

Astropy Collaboration, Price-Whelan, A. M., Sipőcz, B. M., et al. 2018, AJ, 156, 123, doi: http://doi.org/10.3847/1538-3881/aabc4f10.3847/1538-3881/aabc4f

Casali, M., Adamson, A., Alves de Oliveira, C., et al. 2007, A&A, 467, 777, doi: http://doi.org/10.1051/0004-6361:2006651410.1051/0004-6361:20066514

Coleman, G. A. L., & Haworth, T. J. 2020, MNRAS, 496, L111, doi: http://doi.org/10.1093/mnrasl/slaa09810.1093/mnrasl/slaa098

Cruz, K. L., Reid, I. N., Liebert, J., Kirkpatrick, J. D., & Lowrance, P. J. 2003, The Astronomical Journal, 126, 2421, doi: http://doi.org/10.1086/37860710.1086/378607

Cutri, R. M., Skrutskie, M. F., van Dyk, S., et al. 2003, VizieR Online Data Catalog, II/246

Fedele, D., van den Ancker, M. E., Petr-Gotzens, M. G., & Rafanelli, P. 2007, A&A, 472, 207, doi: http://doi.org/10.1051/0004-6361:2007772510.1051/0004-6361:20077725

Haisch, Karl E., J., Lada, E. A., & Lada, C. J. 2001, ApJ, 553, L153, doi: http://doi.org/10.1086/32068510.1086/320685

Harris, C. R., Millman, K. J., van der Walt, S. J., et al. 2020, Nature, 585, 357, doi: http://doi.org/10.1038/s41586-020-2649-210.1038/s41586-020-2649-2

Herbst, W., LeDuc, K., Hamilton, C. M., et al. 2010, The Astronomical Journal, 140, 2025, doi: http://doi.org/10.1088/0004-6256/140/6/202510.1088/0004-6256/140/6/2025

Lada, C. J., & Wilking, B. A. 1984, ApJ, 287, 610, doi: http://doi.org/10.1086/16271910.1086/162719

Lawrence, A., Warren, S. J., Almaini, O., et al. 2007, MNRAS, 379, 1599, doi: http://doi.org/10.1111/j.1365-2966.2007.12040.x10.1111/j.1365-2966.2007.12040.x

Manara, C. F., Ansdell, M., Rosotti, G. P., et al. 2022, arXiv e-prints, arXiv:2203.09930. https://arxiv.org/abs/2203.09930https://arxiv.org/abs/2203.09930

Plavchan, P., Gee, A. H., Stapelfeldt, K., & Becker, A. 2008, ApJ, 684, L37, doi: http://doi.org/10.1086/59210710.1086/592107

Plavchan, P., Güth, T., Laohakunakorn, N., & Parks, J. R. 2013, A&A, 554, A110, doi: http://doi.org/10.1051/0004-6361/20122074710.1051/0004-6361/201220747

Rebull, L. M., Cody, A. M., Covey, K. R., et al. 2014, AJ, 148, 92, doi: http://doi.org/10.1088/0004-6256/148/5/9210.1088/0004-6256/148/5/92

Silverberg, S. M., Wisniewski, J. P., Kuchner, M. J., et al. 2020, The Astrophysical Journal, 890, 106, doi: http://doi.org/10.3847/1538-4357/ab68e610.3847/1538-4357/ab68e6

The Astropy Collaboration, Price-Whelan, A. M., Lian Lim, P., et al. 2022, arXiv e-prints, arXiv:2206.14220. https://arxiv.org/abs/2206.14220https://arxiv.org/abs/2206.14220

Williams, J. P., & Cieza, L. A. 2011, ARA&A, 49, 67, doi: http://doi.org/10.1146/annurev-astro-081710-10254810.1146/annurev-astro-081710-102548

A.. Appendix

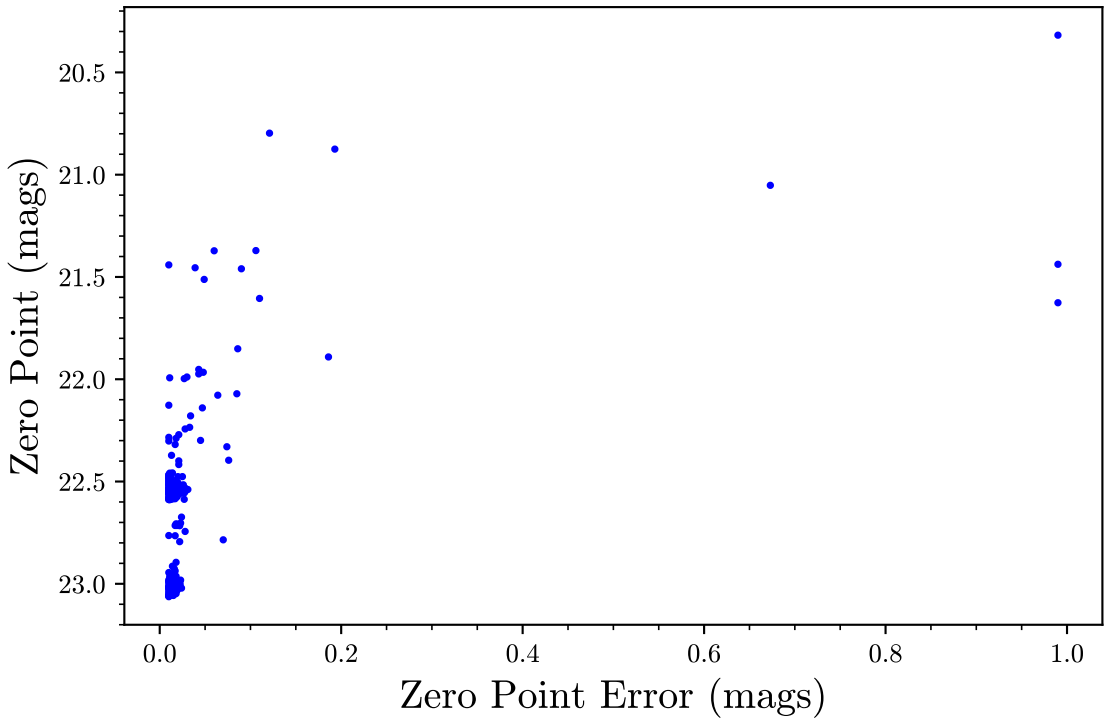

Figure A.1: Zero point vs. its corresponding error. This shows that, for the most part, the error on the zero point was significantly less than the value for the zero point. Since all of the errors were, for the most part, very reasonable, no data needed to be rejected by poor zeropoint value alone for the final light curves in Figures 5 and 6.

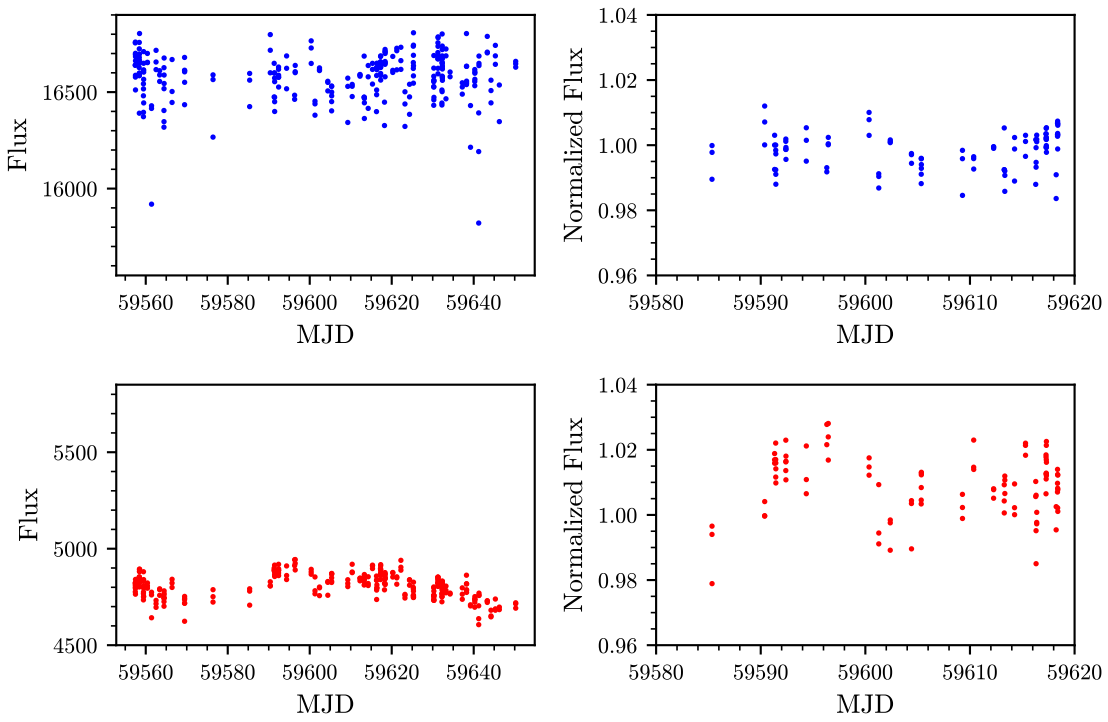

Figure A.2: Field star corrected as well as our target stars' light curves. The top left and top right figures show the field star, and the bottom left and bottom right figures show 2MASS J0619-2903. The two left figures are showing the raw flux curve after the corrections outlined in 2.1 were made. The two plots on the right show a normalized flux by dividing by the median of each respective curve. From the plots, it is evident that 2MASS J0619-2903 has variability on days-long timescales.